Estimate of repulsive interatomic pair potentials by low-energy alkali-metal-ion scattering and computer simulation

R. Ghrayeb
Université Libre de Bruxelles, Campus de la Plaine, (Code Postale 234), Boulevard du Triomphe, B-1050 Bruxelles, Belgium

M. Purushotham
Technische Universität Clausthal, Leibnitzstrasse 4, D-3392 Clausthal-Zellerfeld, Federal Republic of Germany

M. Hou
Université Libre de Bruxelles, Campus de la Plaine, (Code Postale 234), Boulevard du Triomphe, B-1050 Bruxelles, Belgium

E. Bauer
Technische Universität Clausthal, Leibnitzstrasse 4, D-3392 Clausthal-Zellerfeld, Federal Republic of Germany
(Received 17 June 1987)

Low-energy ion scattering is used in combination with computer simulation to study the interaction potential between 600-eV potassium ions and atoms in metallic surfaces. A special algorithm is described which is used with the computer simulation code MARLOWE. This algorithm builds up impact areas on the simulated solid surface from which scattering cross sections can be estimated with an accuracy better than 1%. This can be done by calculating no more than a couple of thousand trajectories. The screening length in the Molière approximation to the Thomas-Fermi potential is fitted in such a way that the ratio between the calculated cross sections for double and single scattering matches the scattering intensity ratio measured experimentally and associated with the same mechanisms. The consistency of the method is checked by repeating the procedure for different incidence conditions and also by predicting the intensities associated with other surface scattering mechanisms. The screening length estimates are found to be insensitive to thermal vibrations. The calculated ratios between scattering cross sections by different processes are suggested to be sensitive enough to the relative atomic positions in order to be useful in surface-structure characterization.

I. INTRODUCTION

Low-energy ion scattering (LEIS) is a surface chemical- and structural-analysis technique which is quite extensively used, both for routine characterization and fundamental research. The basic process in LEIS is the interaction between a slowing-down ion and the atoms close to the solid surface. The interaction is governed by the interatomic potential, the modeling of which still causes problems.

On the other hand, when the ion scattering is the consequence of only very few successive collisions, a kinematic analysis may be sufficient to understand the gross structure of experimental energy dispersion spectra. Computer simulation may be useful, therefore. An accurate knowledge of the atomic interaction potential is not necessary as long as the energy lost in the scattering process gives sufficient information; for example, in qualitative or—after calibration—in quantitative chemical analysis.[1] However, for quantitative structural analysis, the intensity is also needed.[2,3] Scattered ion flux studies became of interest as a consequence of the discovery of "wedge focusing," which consists in an increase of the flux of ion trajectories at the edge of the area shadowed by a target atom.[4] This limiting area was identified as a "shadow cone." This flux enhancement was first used in surface-structure analysis with medium-energy light ions as a probe.[5]

Later on, the method was found particularly promising in LEIS (Refs. 1–3) and the possibilities of the method were enhanced. The scattered fluxes are directly related to the differential scattering cross sections and thus to the interatomic potential. Therefore, the understanding of all peak intensities in LEIS energy distributions requires the knowledge of the potential. Until now, more attention has been paid to the shape of the shadow cone than to intensities, although the latter are usually quite sensitive to the relative atomic positions. Thus provided a good knowledge of the potential is attained, LEIS can be used for surface-structure analysis, just by comparing the relative experimental intensities to the predictions of the calculations. Conversely, when the scattering occurs from well-defined surfaces, the same comparison may allow to estimate the interaction

potential.

In the present work it will be shown how the comparison between LEIS experiments with alkali-metal ions on metals with computer simulations allows us to estimate pair potentials with remarkable accuracy, without prohibitive numerical calculations.

II. THE INTERATOMIC POTENTIAL

Model potentials are usually given in the form of universal functions whose analytical expressions include a dependence on the atomic number of the interacting atoms and their distance. As it is desirable that the potential function is applicable to the widest energy range as well, Thomas-Fermi-like models that include an asymptotic coulombian distance dependence are quite popular. A particularly convenient form was suggested by Molière.[6] It may be written as

$$V(r)=(Z_1Z_2e^2/r)\Phi(r/a)\ , \tag{1a}$$

with the screening function

$$\Phi(r/a)=0.35\exp(-0.3r/a)+0.55\exp(-1.2r/a)+0.1\exp(-6.0r/a)\ , \tag{1b}$$

where r is the interatomic distance and a the adjustable screening length. The form of the screening function has the advantage to include only one parameter and to require the calculation of only one exponential term for each collision, thus allowing fast computation. General expressions were suggested by Firsov[7] and Lindhard[8] for the screening length, which are not sufficiently accurate for the purpose of scattering intensity comparison in LEIS.

Another semiempirical potential model was suggested more recently. It was obtained as a least-square fit to many pair potentials evaluated by selfconsistant calculations with nonrelativistic wave functions.[9] It is known as the "universal potential." For many interacting pairs, the screening function of the "universal" potential deviates significantly from (1) when evaluated with the Firsov screening length. A correction factor to Firsov depending only on the atomic numbers of the interacting atoms has been suggested,[10] which brings (1) rather close to the universal potential function and thus provides similar scattering cross sections.

III. THE METHOD

The MARLOWE computer program is used to perform the simulations.[11] The trajectories of the moving atoms are calculated as sequences of binary collisions until either they escape the target surface or their kinetic energy falls below some cutoff value. Provision is made for an approximate model for quasisimultaneous collisions[12] which preserves momentum and scales the energies. Since only the incident atom trajectories are of interest in ion scattering, no target atom displacement is calculated.

The modular structure of the MARLOWE code allows additional or alternative procedures to control any aspect of the trajectory calculations. Thus it was possible to append an analysis routine closely simulating the experimental detection conditions. It was already used in Ref. 13. In addition, a feedback was installed between the analysis routine and the initialization procedure. This allows to select the initial impact point of the next projectile on the surface with regard to the fate of the previously scattered one. This saves a large amount of computer time in the way described below.

In order to test potentials, we compare relative intensities obtained from LEIS experiments with the results of computer simulations, using various values of the screening length in the Molière potential. Alkali-metal ions are used for the scattering from metal surfaces with work functions large enough to avoid neutralization. Matching of the experimental peak ratios to the simulation results allows us to estimate the screening parameter in (1) with an accuracy of better than 0.2%.

However, computer simulations of a homogeneous incident ion beam have to be performed with such good statistics that no presently available computer would be fast enough to estimate a peak ratio within 1% in less than one month.

Therefore, another method was developed which allows the computation of scattering cross sections with the same accuracy whatever the scattering probability is. No more than a few thousand ion trajectories need to be calculated to determine the scattering cross section for a specific mechanism within an accuracy better than 1%.

Considering the scattering by one process within a specific solid angle and energy interval, the method is based on the determination of the impact area on the surface which gives rise to the scattering with the specified conditions.

The algorithm is sketched in Fig. 1 and works as follows: Consider point C outside the target from which a projectile is initiated, giving rise to the scattering in the desired conditions. This point is surrounded by a contour delimiting the area in which all initiated projectiles will undergo the scattering in the desired conditions [Fig. 1(a)]. From point C, a pointer is moved stepwise in a given direction and a projectile is initiated at each step, until the edge of the area is encountered. Two points, A_1 and B_1 are thus defined, which are the last belonging to the impact zone and the first which does not, respectively. From these, the complete contour is mapped by triangulation and the points A_i $(i=1,\ldots,n)$ and B_j $(j=1,\ldots,m)$ are determined inside and outside the contour, according to the specified scattering conditions. Default and excess estimates of the delimited area, S, can easily be computed, using the vector products between the vectors joining point C to the points of types A and B:

$$\sum_{i=1}^{n} |\mathbf{r}_{CA_i}\times\mathbf{r}_{CA_{i+1}}| < 2S < \sum_{j=1}^{m} |\mathbf{r}_{CB_j}\times\mathbf{r}_{CB_{j+1}}|\ , \tag{2}$$

where n and m are the total number of points of type A and B required to close the mapping of the contour.

In such a way, the accuracy of the estimate of the impact area—and thus the scattering intensity—only depends on the step size of the mapping and is automatically estimated. It is independent of the size of the area.

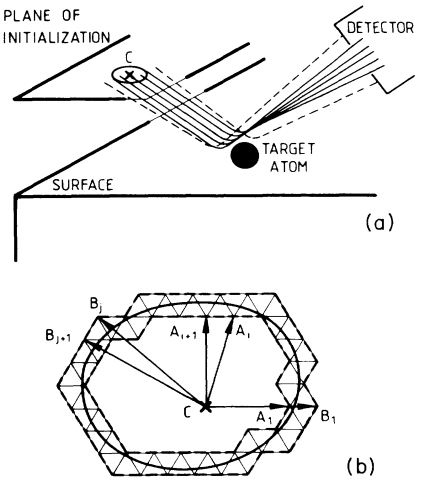

FIG. 1. Determination of impact areas. (a) Projectiles are initialized in a plane outside the target surface. Those initialized in the area around point C penetrate the detector after some scattering process at the surface (solid lines). The others do not (dashed lines). (b) In order to determine the impact area, a pointer is started from C and is moved along a straight line. Points A_1 and B_1 are localized. A_1 is the last inside the impact area and B_1 is the first outside. Vectors entering relation (2) in the text are drawn. The solid line represents the exact contour, the dashed lines represent the computed contours as used for the under and over estimates of the exact impact area.

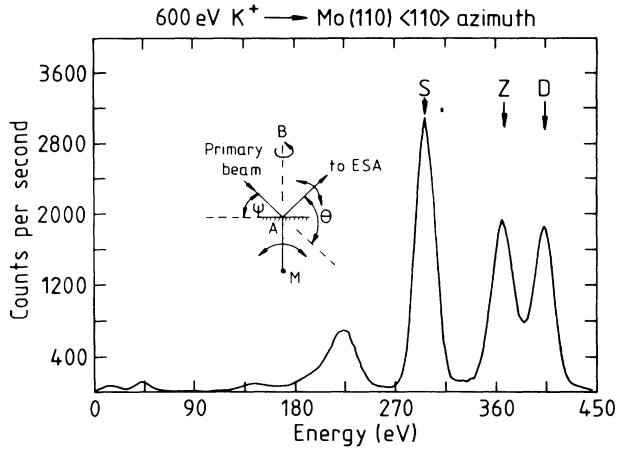

FIG. 2. Typical energy dispersion spectrum as obtained from LEIS experiments. Projectiles are 600-eV K^+ ions. The scattering geometry is shown in the inset. ψ is the sliding angle and θ the scattering angle. The target can be rotated around axes A (in the surface plane), B (dashed line), and M. The electrostatic analyzer (ESA) can be rotated in the plane of incidence around axis A. Potassium ions are incident on a Mo(110) surface at a sliding angle $\psi=40°$. The plane of incidence is parallel to a ⟨110⟩ surface direction and the detector is located in the specular direction. The labels above the peaks quote the attributed scattering mechanisms: S, single; D, double; Z, zig-zag.

IV. EXPERIMENTAL CONDITIONS

The measurements were done in an ultrahigh vacuum (UHV) system with a base pressure of 4×10^{-11} mbar. In addition to the low-energy ion scattering spectrometer (LEISS), it is equipped with an Auger-electron spectrometer (AES), low-energy electron diffraction (LEED) optics, a quadrupole mass spectrometer, and several evaporators whose rate is well calibrated by AES and LEED. The LEISS consists of an alkali-metal ion gun, a rotatable 127° electrostatic analyzer (ESA), and a three-axis rotatable crystal manipulator. The ion beam passes through a Wien filter in order to separate out impurity ions and neutrals. The change in beam current was less than 2% over a measurement period of 8 h. The beam diameter on the target is 1.5 mm. The ESA has a nearly flat transmission of 48% from 50 eV to 2 keV. It has an angular resolution of 1° and an energy resolution of 1.6%. The scattering geometry is shown in the inset of Fig. 2. The target manipulator allows one rotation about a major axis M to facilitate various measurements (LEED, AES, etc.). The polar angle of incidence can be changed by rotating the crystal about an axis A in the surface plane of the crystal and perpendicular to the plane of incidence. The total scattering angle can be changed by rotating the ESA around the same axis A. The azimuth is changed by rotating the crystal about an axis B normal to the crystal surface and in the scattering plane. The various angles can be determined within an accuracy of 0.5°. The primary beam current can be measured by swinging a Faraday cup in the path of the ion beam. Before and after the measurements, the chemical cleanliness of the target was controlled by AES and the structure by LEED.

The initial cleaning of the Mo single crystal was done in the usual procedure by repeating annealing at about 1300 K in an oxygen partial pressure of about 5×10^{-6} mbar followed by flashing to about 2000 K. The crystal was orientated to within 0.05° of the (110) plane. After the initial cleaning, no contamination could be detected either by AES or by LEISS. Measurements were done on the freshly annealed Mo(110) surface or well characterized metal layers. Beam currents of the order of 1 nA were used during the measurements and controlled in between. To ensure equal ion dose for single and multiple scattering peaks, the energy was scanned once in 10 sec. Six to ten scans were added up to make one spectrum. Several spectra were collected with the same scattering conditions and added up to reduce the statistical error. No damage due to ion bombardment during the measurement could be detected either with AES or with LEISS. A new surface was prepared for every individual spectrum by flashing the crystal to about 2000 K in order to desorb CO and the alkalis which might have been absorbed during the preceding measurement.

The different evaporators were calibrated by the breaks in the AES peak to peak amplitudes of the overlayers on Mo(110) as a function of time.[14] Approximate-

ly one and two monolayers thick Cu films were used for the LEISS measurements. Although no sputtering was observable either by AES or by LEISS during the recording of a single spectrum, each freshly prepared layer was used for every spectrum. The Cu layers were annealed at about 600 K to achieve a smooth surface. In the case of Au and Ag the layers were prepared by evaporation onto well prepared and characterized Cu films about 1 monolayer in thickness rather than on clean Mo(110) in order to obtain a single overlayer. To minimize ion beam mixing a fresh prepared layer was used for every spectrum as in the case of Cu and Mo.

V. THE RESULTS

A typical experimental spectrum obtained for the scattering of potassium ions from a Mo(110) surface is given in Fig. 2. By a straightforward kinematic analysis, the main peak is found to result from a single surface collision and the highest energy peak can be attributed to a two-dimensional double scattering event. The peak inbetween is typical of a zig-zag collision, and the lower energy peaks were found on tungsten to result from more complex scattering processes. They could be identified with the help of computer simulation.[13]

Knowing the leading edge of the double collision peak and assuming that it should be symmetric, its separation from the zig-zag peak can be done quite reasonably and the associated intensities can than be estimated. Since the energy filter is an electrostatic analyzer, the energy window is proportional to the input energy and care was taken in the design of the entrance and exit slits so that no other parameter has a significant influence on its transmission. Therefore, the ratio between the differential cross sections for double and single scattering can reasonably be estimated as

$$R_{DS}=(I_D/I_S)(\Delta E_S/\Delta E_D)\ , \tag{3}$$

where I_D and I_S are the intensities measured in the double and single collision peaks, and ΔE_D and ΔE_S are the corresponding instrumental energy windows. R_{DS} can be directly compared with the ratio between the impact areas obtained in simulations.

The computed ratio, for the same incidence condition and exit solid angle, is shown in Fig. 3 as a function of the screening length. As, according to (2), the theoretical uncertainties are not sufficiently large to be distinguishable in the figure, the relation between relative peak heights and screening lengths can be made extremely accurately. Therefore, the experimental uncertainties dominate in the screening length determination. In Fig. 3 the peak ratios anticipated from the "corrected" and uncorrected Firsov screening distances are found to be quite distinct from each other as well as from the experimental value. The method thus appears to be quite discriminative in the potential determination.

Calculations and measurements were repeated with well-known surfaces of different materials. The results are given in Table I and compared with the corrected and uncorrected Firsov screening lengths. In order to check the consistency of the method, the same screening length determination was repeated for different scattering angles ranging from 80° to 120° in specular conditions. Screening lengths were deduced from the peak ratios R_{DS}, between double and single and R_{DZ}, between the double and zig-zag collision peaks. All screening lengths found for the potassium-molybdenum interaction pair were between 0.0954 and 0.0957 Å. This interval of 3×10^{-4} Å represents the uncertainty inherent to the method.

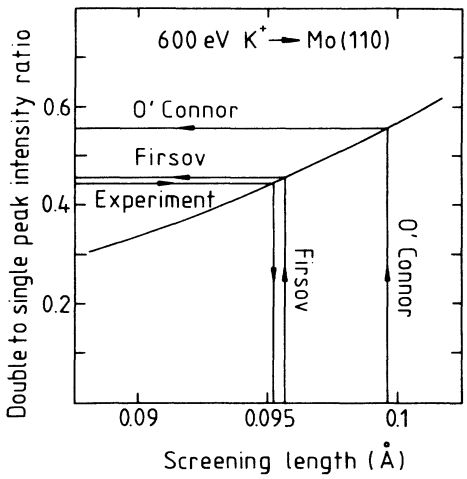

FIG. 3. Double to single scattering intensity ratio as a function of the screening length used in the simulations. The incidence conditions are the same as in Fig. 2. It is shown how the experimental peak ratio allows us to determine the screening length. The comparison with the ratios predicted when using Firsov and O'Connor's values shows how the method helps in discriminating between potentials.

VI. DISCUSSION

A. The potential

The potassium-molybdenum potential was already estimated in a previous study on the basis of experimental measurements and computer simulation.[15] As the method of the authors is different from ours, a comparison is useful. They measured the reflection intensity of various types of alkali-metal ions from ⟨110⟩ atomic chains in a (001) molybdenum surface. For a fixed analyzer position, the scattered intensity increases as the angle between the incidence direction and the chains decreases and it drops off suddenly at some critical angle below which shadowing occurs.[15] This critical angle is potential dependent and a comparison between its experimental value and computer evaluations allows to determine the potential parameter.

Close to the critical angle (typically less than 20°) the intensity dependence is quite sensitive to thermal displacements and lattice defects. Therefore, the cutoff tends to be smoother than calculated for a perfect static lattice. The comparison with the present estimate is, however, excellent, showing that such an uncertainty

TABLE I. Screening lengths (in Å) for the Molière potential.

Interacting pair	K-Ag	K-Au	K-Cu	K-Mo	K-W
Firsov	0.0935	0.0837	0.1027	0.0962	0.085
O'Connor	0.0972	0.0951	0.1005	0.0991	0.0952
This work	0.0795	0.0823	0.0902	0.0955	0.0984

does not affect the results too much.

It is striking that the discrepancies between the present estimates of screening distances and those deduced by Firsov or O'Connor[7,10] are not systematic. This suggests that there is no monotonic dependence of the screening length on the atomic numbers of the interacting atoms. This is qualitatively consistent with the fluctuations in the screening functions estimated by selfconsistant calculations, from which a least-squares fit was considered to represent a universal function. It should be noticed as well that there are additional uncertainties concerning the functional dependence of the screening function on the interaction distance. As this distance was not controlled in the present work, the determination of potentials made here may only be valid for distances typical for single and double scattering at energies of a few hundred electron volts. Three sources of uncertainties need to be considered in the present results, which we believe to be of negligible influence. These are the effect of thermal displacements, ion neutralization, and peak overlap deconvolution problems.

B. Thermal displacements

The intensity of single scattering is not expected to be influenced by surface atomic displacements as it only depends on the density of scattering centers and not on their positions. The situation is a little more delicate in double scattering since the associated scattered intensity depends on the relative atomic positions.

We believe that our method is not as sensitive to thermal displacements than the critical shadowing angle method. Whether the second atom in a chain is shadowed or not depends on the exact position of the first scattering center. A characteristic distance in such an impact process is the distance of closest approach in a head-on collision, which is of the same order of magnitude as the root-mean-square thermal displacement of a surface atom. In our experiments the angle between any surface direction and the incident beam is significantly larger (40°–60°) and such chain effects are not expected to play a role and, therefore, our results should not be affected by thermal vibrations. Qualitatively, this can be understood on the basis of the following argument.

Consider the situation of the double scattering in the case of an incidence direction close to the normal at the surface. No surface chain effect can then be expected. The scattered intensity from the first collision is independent of the atomic position and the azimuthal distribution of the scattered intensity is close to isotropic. Therefore, the scattered intensity from the second atom will not be affected by small displacements from its lattice site. Indeed, as the root-mean-square thermal displacements are typically more than an order of magnitude smaller than the first-neighbor distance, the effect of thermal displacements of the two scattering atoms at distances once smaller and once larger than the equilibrium distance will balance to some extent.

This argument does not take into account the correlations in the thermal displacements that still reduce their effect. It is not rigorous, however, but it is supported by three experimental facts and computer simulation. First, relative thermal displacements have the effect of modifying the successive scattering angles—and thus the scattering energies—and consequently the double scattering peak would occur at lower energy than expected from the kinematics. If this effect takes place, it is beyond the resolution possibilities of our experimental spectra and can thus be suggested to have negligible influence on our peak ratio measurements. Second, the effect may be expected to be different for double collisions in the plane of incidence and for zig-zag collisions. Both processes, however, were found to lead to remarkably similar screening length estimates. The same argument holds for the double scattering process at different scattering angles. Third, in a previous study the effect of temperature was measured in the case of scattering from tungsten of potassium, using the same incidence geometry.[16] A systematic reduction of the intensities, of the order of 20%, was found with temperature increasing from room temperature to twice this value. The exact reason for this decrease is still not fully understood, but the peak ratios remain unchanged, also suggesting that the present estimates are not significantly influenced by thermal vibrations.

Finally, computer intensity calculations were performed using different relative positions of the second atom position with respect to the first. These were performed for several displacements typical of thermal vibrations in three orthogonal directions. Two directions were considered in the surface, respectively, parallel and orthogonal to the plane of incidence, and the third, normal to the surface. Displacement orthogonal to the plane of incidence was found to have no significant influence on the double scattering intensity. It was significant, however, for displacements in the two other directions, but the variation of the peak intensities when the second atom is displaced toward one or the other side of its equilibrium position were found to balance almost exactly.

C. Neutralization

The charge fraction of alkali-metal atoms scattered from a metal surface is a decreasing function of the energy.[17] It is the highest, however, for potassium and was found above 0.999 when scattered from a copper surface.

As the work functions of the metal surfaces used in the present study are similar or larger than that of copper, the neutralization of potassium can reasonably be neglected without affecting the accuracy of the screening length estimates.

Since, in the case of other alkali-metal ions, the charge fraction was found to be trajectory independent,[17,18] the peak ratios are unaffected by the charge exchanges between the ions and the surface. As a consequence, the potential determination method presented here is also adequate for other alkali-metal ions than potassium.

D. Peak overlaps

The potential determination was carried on by using incidence and detection conditions such that single, zig-zag, and double scattering in the plane of incidence produce well-separated peaks in the energy distributions. In many circumstances, however, this is not the case. It is even sometimes impossible to identify the different scattering mechanisms that contribute to the structures in the energy distributions.

A typical example is given in Fig. 4. This energy distribution was obtained for potassium ions scattered from a Ag(111) surface. The plane of incidence was kept parallel to a ⟨112⟩ surface direction. The gross structure looks similar to that shown in Fig. 2, except the larger width of the high-energy peak. However, the peak intensity ratio is about twice as much as predicted by the calculation of the double to single scattering intensities when using the same screening length as estimated previously, with the plane of incidence parallel to a ⟨110⟩ surface direction. This is a clear indication that additional mechanisms contribute to the same peak. A careful simulation revealed the occurrence of two mechanisms contributing to the same peak. These are drawn in the inset of Fig. 4. Only the zig-zag double scattering process was found to contribute to the intermediate-energy peak.

If computer simulation shows evidence for several scattering processes, these are not necessarily the *only* occurring ones. The impact area method described above allows us, however, to calculate the exact contribution of each mechanism to each peak. When this is done, the calculated peak intensity ratios, only including the mechanisms shown in the insets of Fig. 4, reproduce the experimental values within the same accuracy as obtained with the ⟨110⟩ azimuthal incidence direction on Mo(110) (Fig. 3). Thus one can conclude that no other scattering process contributes significantly to the peaks observed in the energy distribution in Fig. 4. The situation of Fig. 4 is typical for all energy distributions obtained for fcc and bcc metals, when the plane of incidence is parallel to a ⟨112⟩ surface direction.

In addition, as already shown in Ref. 13, contributions of the scattering from the second layer may take place

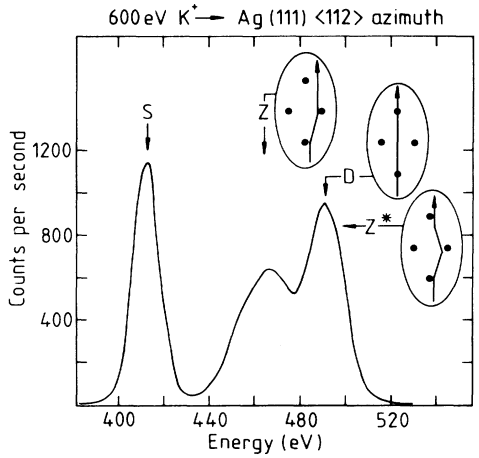

FIG. 4. Energy dispersion spectrum. Projectiles are 600-eV K^+-ions. They are incident on a Ag(111) surface at a sliding angle $\psi = 30°$. The plane of incidence is parallel to a ⟨112⟩ surface direction and the detector is located in the specular direction. The peak labels, *S*, *Z*, and *D* have the same meaning as in Fig. 2. An additional mechanism labeled Z^* contributes to the highest energy peak, which cannot be resolved without computer simulation. The scattering processes *Z*, Z^*, and *D* are plotted in the insets.

when the incidence angle is close enough to the surface normal. They can be estimated by the same impact area method.

VII. CONCLUSIONS

The combination of experimental LEIS and computer simulation using the impact area method proves to be quite efficient in the potential parameter determination. However, in the discussion, we implicitly assume the screening length function $1b$ to have the correct distance dependence. This is questionable and deviations from the exponential law are discussed elsewhere.[10] It may thus well be that the same screening parameter method at other energies leads to different screening length estimates. This suggests that a further step in the potential determination can be made by repeating the procedure for a wide range of incidence energies. The relation between the energy and the distance of closest approach in a collision could then allow us to build more accurate screening functions. In the present study the impact area method was applied to the scattering from surfaces with well-known lattice constants.

On the other hand, small changes in the first-neighbor distance may induce significant changes in the peak ratios. A matching procedure between simulation and experimental peak ratios, using the neighbor distance as a parameter, can thus be expected to provide useful information about overlayer structures.

[1]W. Heiland and E. Taglauer, Methods Exp. Phys. **22**, 299 (1985).

[2]E. Bauer and T. Von dem Hagen, in *Chemistry and Physics of Solid Surfaces IV*, edited by R. Vanselow and R. Howe (Springer, Berlin, 1986), p. 547.

[3]H. Niehus, J. Vac. Sci. Technol. (to be published).

[4]H. H. W. Feijen, Ph.D. thesis, University of Groningen, 1975, pp. 53–109 (unpublished).

[5]W. C. Turkenburg, W. Soszka, F. W. Saris, H. H. Kersten, and B. G. Colenbrander, Nucl. Instrum. Methods **132**, 587 (1976).
[6]G. Molière, Z. Naturforsch. A **2**, 133 (1947).
[7]O. B. Firsov, Zh. Eksp. Teor. Fiz. **33**, 696 (1958) [Sov. Phys.—JETP **6**, 534 (1958)].
[8]J. Lindhard, K. Dans. Vidensk. Selsk. Mat. Fys. Medd. **34**, 14 (1965).
[9]F. Ziegler, J. P. Biersack, and U. Litmark, Oak Ridge National Laboratory Report No. CONF-820131 (unpublished).
[10]J. O'Connor and J. P. Biersack, Nucl. Instrum. Methods **B15**, 14 (1986).
[11]M. T. Robinson and I. M. Torrens, Phys. Rev. B **9**, 5008 (1976).
[12]M. Hou and M. T. Robinson, Nucl. Instrum. Methods **132**, 641 (1976).
[13]T. Von dem Hagen, M. Hou, and E. Bauer, Surf. Sci. **117**, 134 (1982).
[14]E. Bauer, H. Poppa, G. Todd, and F. Bonczek, J. Appl. Phys. **45**, 5164 (1974).
[15]S. H. Overbury and R. H. Huntley, Phys. Rev. B **32**, 10 (1985); **32**, 6278 (1985).
[16]T. Von dem Hagen, thesis, Technische Universität Clausthal, 1982 (unpublished).
[17]A. J. Algra, thesis, University of Groningen, 1981 (unpublished).
[18]A. Boers, Surf. Sci. **63**, 475 (1977).